

Honeycomb-Patterned Photoluminescent Films Fabricated by Self-Assembly of Hyperbranched Polymers**

Cuihua Liu, Chao Gao,* and Deyue Yan*

Honeycomb-patterned films made by the self-assembly of polymers have aroused increasing interest because of their fascinating morphology and potential applications.^[1–3] Although much of the work has focused on linear^[1–13] and star-shaped^[1,4] macromolecules, the use of dendritic polymers, with their three-dimensional architectures and unique properties, significantly enlarges the structural diversity and makes multifunctional self-assembly accessible.^[14] The combination of supramolecular chemistry and nanotechnology has recently offered an alternative approach to functional self-assembly. Quantum dots (for example, CdSe)^[3] and fullerenes^[15] have been mixed with polymers to fabricate luminescent honeycomb films. However, the dispersibility of nanomaterials in a polymer matrix is limited, which results in their random distribution in the organized films. It is quite difficult to achieve a dispersion of one substance in another one at a molecular level simply by mixing because of aggregation. To meet this challenge and explore a new area of functional self-assembly, we have shifted our attention from conventional linear macromolecules to hyperbranched polymers.

Hyperbranched polymers play a very important role in self-assembly and greatly enrich the range of host materials and building blocks that can be used in supramolecular chemistry.^[14,16–18] So far, nanofibers,^[16] giant vesicles,^[17] and visible tubes^[18] have been obtained by the self-assembly of amphiphilic hyperbranched polymers in a solvent. Intriguingly, a core-shell amphiphilic dendritic macromolecule can be regarded as a unimolecular micelle or nanobox^[19–21] in which small guests, such as dyes, quantum dots, and noble metals, can be loaded.^[21–23] This property generates the ability

for the molecular-level dispersion and distribution of one or even more substances in another one.

Accordingly, multifunctional assembled structures would be expected to have applications as the junctions of honeycomb-patterned films, in dendritic polymers, and in host-guest chemistry. Herein, we report that honeycomb-patterned films with thicknesses ranging from tens of nanometers to micrometers can be prepared by the molecular self-assembly of amphiphilic hyperbranched poly(amidoamine)s (HPAMAMs). Moreover, the HPAMAMs can encapsulate dye molecules to form colorful host-guest supramolecular complexes. Various luminescent honeycomb-patterned films with tunable emission wavelengths (λ_{em}) were prepared by subsequent nonmolecular self-assembly of the complex on substrates.

An amphiphilic hyperbranched polymer, poly(amidoamine) modified with palmitoyl chloride (HPAMAM10K-C16; see the Supporting Information),^[23] was chosen as the first material for the construction of the porous films. The films were prepared by dropping a solution of the HPAMAM10K-C16 in chloroform on to a cleaned substrate (for example, a silicon wafer, quartz, mica, etc.) and then analyzed by SEM, AFM, TEM, and optical fluorescence microscopy (see the Supporting Information). Figure 1 a–c shows representative SEM images of a HPAMAM10K-C16 film on a silicon wafer. The film contains highly ordered arrays of

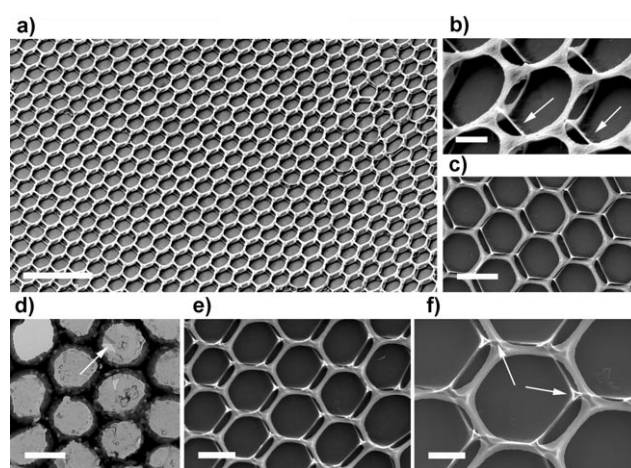


Figure 1. Representative SEM and TEM images of the honeycomb-patterned films on a silicon wafer. a)–c) SEM images of the film prepared from HPAMAM10K-C16; the sample was tilted 45° in the images of (a) and (b). d) TEM image of the film, showing the bottom ultrathin film at the broken sites. e) and f) SEM images of the CR-loaded HPAMAM10K-C16 film. The accelerating voltage was 5 kV for (a) and (b), 20 kV for (c), and 30 kV for (e) and (f). The scale bars are 20 μm (a), 2 μm (b), 5 μm (c), 5 μm (d), 2 μm (e), and 1 μm (f).

[*] Dr. C. Liu, Dr. C. Gao, Prof. D. Yan
College of Chemistry and Chemical Engineering
State Key Laboratory of Metal Matrix Composites
Shanghai Jiao Tong University
800 Dongchuan Road, Shanghai 200240 (P.R. China)
Fax: (+86) 21-5474-1297
E-mail: chaogao@sjtu.edu.cn
dyyan@sjtu.edu.cn

[**] Financial support from the National Basic Research Program (2007CB808000), the National Natural Science Foundation of China (nos. 20304007, 50473010, and 50633010), the Program for New Century Excellent Talents in University, the Foundation for the Author of National Excellent Doctoral Dissertation of China (no. 200527), and the Fok Ying Tung Education Foundation (no. 91013) are greatly appreciated. We thank Prof. S. K. Yan and S. D. Jiang in the Institute of Chemistry Chinese Academy of Sciences for helping with the TEM analysis.

Supporting information for this article (including Experimental details) is available on the WWW under <http://www.angewandte.org> or from the author.

honeycomb-patterned holes with a width of 5–6 μm . There are about 410 holes in an area of $125 \times 85 \mu\text{m}^2$ (Figure 1a), and almost all of them are regular and uniform hexagons except for five pentagons and two heptagons (<2% defects). The top view of the SEM image shows that each hexagonal unit resembles a microhoneycomb cell with six double-layered walls (Figure 1b,c). Two techniques were used in the SEM measurements to confirm the structure of the walls: tilting the sample holder and using a high accelerating voltage. The structure of the double-layer walls can be clearly seen from the high-magnification SEM image tilted 45° (Figure 1b). The bottom layer of the walls is connected through an ultrathin film spread on the solid substrate (Figure 1b, arrow). A protuberance is found on each upper corner of the hexagons (Figure 1b). When the voltage is higher than 20 kV, the skeleton of the bottom layer can also be observed covered by the top layer (Figure 1c). The structures of the patterned films were also confirmed by TEM (Figure 1d). The bottom ultrathin film can be clearly observed at the destroyed sites made by tearing the film off the substrate (see arrow).

The morphology of the patterned film was also verified by AFM (Figure 2). The structures of the honeycomb films can be clearly discerned from the SEM, TEM, and AFM images. A schematic representation of one honeycomb cell is shown in Figure 2d.

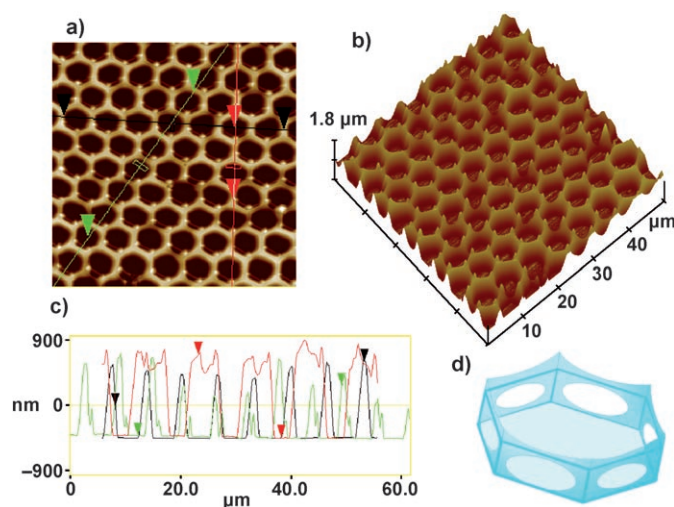


Figure 2. AFM images of the film prepared from HPAMAM10K-C16 on a silicon wafer: a) top view, b) surface plot, c) section analysis of image (a). d) Schematic representation of one honeycomb cell of the film. According to the section analysis, the bottom layer of the wall has a height of about 200 nm (green line, the lower peaks) and the upper layer a height of about 1200 nm (green line, the upper peaks); the upper surface of the walls is arc-shaped and the peaks (the protuberances of corners) are higher than the valleys by about 200 nm (see the red line).

Interestingly, HPAMAM10K-C16 is highly photoluminescent despite the absence of π – π conjugated units (Figure 3). Colorful hexagonal patterns from the assembled film could be observed under the fluorescence microscope (Figure 3a). The patterns are blue and green under excitation wavelengths

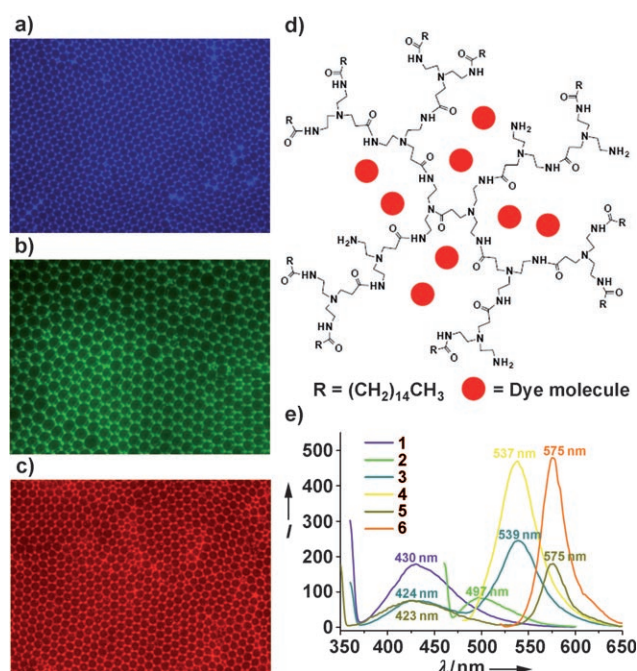


Figure 3. Optical fluorescence microscope images of the film prepared from: a) HPAMAM10K-C16 on a silicon wafer, b) FSS-loaded HPAMAM10K-C16 on quartz, and c) CR-loaded HPAMAM10K-C16 on quartz. d) Schematic illustration of dye-loaded HPAMAM10K-C16. e) Fluorescence spectra of HPAMAM10K-C16 (line 1: $\lambda_{\text{ex}} = 360 \text{ nm}$, line 2: $\lambda_{\text{ex}} = 460 \text{ nm}$), FSS-loaded HPAMAM10K-C16 (line 3: $\lambda_{\text{ex}} = 360 \text{ nm}$, line 4: $\lambda_{\text{ex}} = 480 \text{ nm}$), and PB-loaded HPAMAM10K-C16 in chloroform (line 5: $\lambda_{\text{ex}} = 350 \text{ nm}$, line 6: $\lambda_{\text{ex}} = 520 \text{ nm}$). I : intensity of fluorescence emission. The light filter used in the optical fluorescence microscopy is UV-2A (a), B-2A (b), and G-2A (c), and the magnification is $\times 400$.

(λ_{ex}) of 330–380 nm (using Nikon filter sets UV-2A) and 450–490 nm (B-2A filter), respectively. No fluorescence was observed under excitation at 510–560 nm (G-2A filter).

We also investigated the possible effects of the substrate, humidity, temperature, concentration, solvents, and polymer species on the morphology of the resulting films. Similar morphologies were observed for films formed on other surfaces (for example, quartz, glass, mica, and gold). At 25°C , the honeycomb films can be prepared with the relative humidity (RH) ranging from 30% to 72% (see the Supporting Information). Honeycomb-patterned films were successfully obtained over a wide concentration range (0.05 – 2 g L^{-1} of HPAMAM10K-C16 in CHCl_3). The more concentrated the solution is, the thicker and deeper are the walls of the cells (see the Supporting Information). Amazingly, the depth of the cells can vary over two to three orders of magnitude for the same micrometer-scale cell dimension by adjusting the polymer concentration. The depth is approximately only 65 nm at 0.05 g L^{-1} , but increases to 1400 nm at 2 g L^{-1} . The films formed from a solution of HPAMAM10K-16C in CH_2Cl_2 or CS_2 also show a porous morphology, but the holes are less regular (see the Supporting Information). No porous structures were detected when cosolvents of chloroform and toluene were used (see the Supporting Information). Similar honeycomb films (see the Supporting Informa-

tion) can be readily fabricated from three other amphiphilic HPAMAMs (see the Supporting Information) with different molecular weights. All of these investigations demonstrate the wide generality and high reproducibility of our findings.

Furthermore, we studied the self-assembly behavior of the dye-loaded HPAMAMs on substrates.^[23] Four kinds of dyes (fluorescein sodium (FSS), phloxine B (PB), rose Bengal (RB), and Congo red (CR)) were loaded (Figure 3d and see the Supporting Information). Similar honeycomb-patterned films were obtained and confirmed by SEM (Figure 1e,f), AFM (see the Supporting Information), and fluorescence microscopy measurements (Figure 3b,c). The images obtained using UV-2A, B-2A, and G-2A filters as well as the fluorescence spectra revealed that these films emitted a different fluorescence from the neat HPAMAM10K-C16 film. Under the G-2A filter, for example, red hexagonal

patterns were observed for the CR-loaded (Figure 3c) and FSS-loaded HPAMAM10K-C16, while yellow patterns were evident for PB-loaded or RB-loaded HPAMAM10K-C16. It is noteworthy that the pattern color and emission band for the same dye-loaded HPAMAM10K-C16 can also be tuned by changing the filters or excitation wavelength (Figure 3e).

Figure 4 presents a schematic explanation as to how the ordered porous films form. At first, the polymer solution is dropped and spread on the substrate homogeneously (Figure 4a). As the solvent evaporates, the surrounding water vapor forms small droplets and deposits on the surface of the solution. The presence of the water droplets changes the characteristics of the solvent dramatically: inducing a phase inversion and aggregation of the hydrophobic shell of the core-shell amphiphilic unimolecular micelles (Figure 4b). The condensation of the polymer solution forces the macromolecules to move closer together to form aggregates (Figure 4c), thereby forming walls and pores. The organized film is initially formed suddenly on evaporation of the chloroform, and further regulated and fixed by the slow evaporation of the residual water droplets and the tiny amount of chloroform remaining (Figure 4d). Concomitantly, the condensation of the unimolecular micelles leads to shrinkage and cracking of the walls as a result of the stress, thereby forming walls with two or more layers (Figure 2a,d). The organization process was monitored on-line by using an optical microscope (see the Supporting Information), which enabled the above assembly mechanism to be proposed.

In conclusion, fluorescent honeycomb-patterned films of amphiphilic hyperbranched poly(amidoamine)s were successfully prepared with high reproducibility on various substrates in a wide range of humidities. The thickness of the patterned films can be altered from the nanometer to the micrometer scale simply by changing the polymer concentration. A supramolecular complex self-assembly strategy for the facile fabrication of multifunctional thin films with ordered microporous patterns has been presented and validated by experiments. This strategy greatly enlarges the diversity of structures that can be assembled, opens up a straightforward route to the functionalization of self-assembly structures, and paves the way to nonmolecular self-assembly of several substances which allows one substance to disperse molecularly in another one. The details and applications of the assembled films are in progress and will be reported later.

Received: October 28, 2006

Revised: March 7, 2007

Published online: April 19, 2007

Keywords: dyes/pigments · fluorescence · polymers · porous films · self-assembly

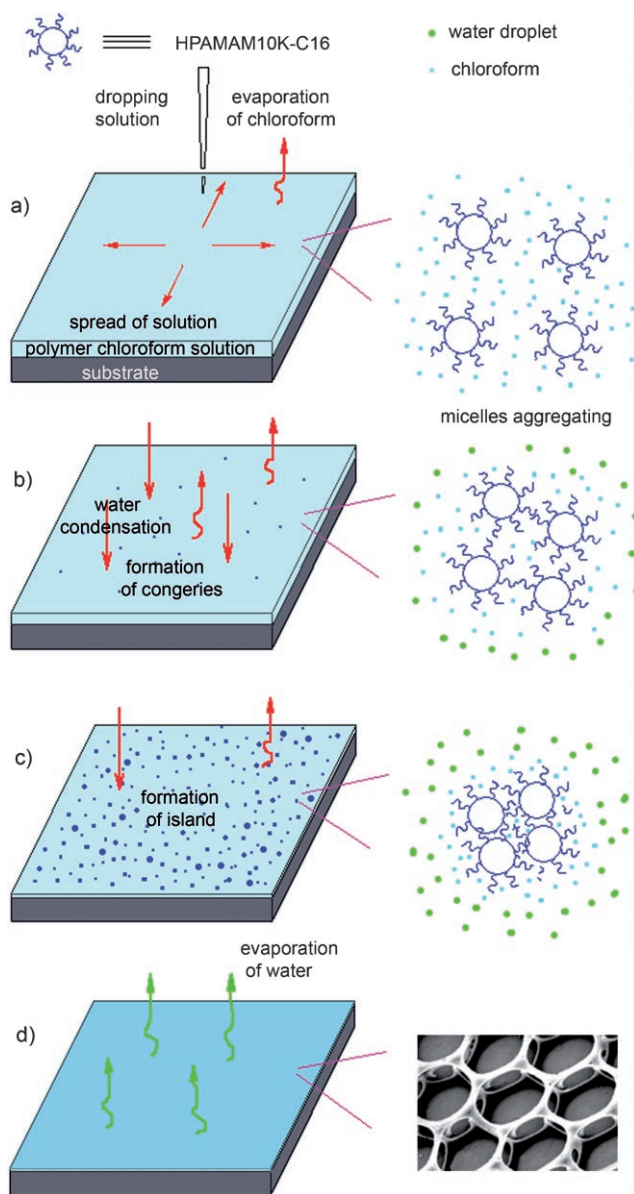


Figure 4. Schematic description of the mechanism for the self-assembly of an amphiphilic hyperbranched polymer on a substrate.

- [1] G. Widawski, M. Rawiso, B. François, *Nature* **1994**, 369, 387–389.
- [2] B. de Boer, U. Stalmach, H. Nijland, G. Hadzioannou, *Adv. Mater.* **2000**, 12, 1581–1583.
- [3] A. Böker, Y. Lin, K. Chiapperini, R. Horowitz, M. Thompson, V. Carreon, T. Xu, C. Abetz, H. Skaiff, A. D. Dinsmore, T. Emrick, T. P. Russell, *Nat. Mater.* **2004**, 3, 302–306.

- [4] B. François, O. Pitois, J. François, *Adv. Mater.* **1995**, 7, 1041–1044.
- [5] N. Maruyama, T. Koito, J. Nishida, T. Sawadaishi, X. Cieren, K. Ijio, O. Karthaus, M. Shimomura, *Thin Solid Films* **1998**, 327–329, 854–856.
- [6] T. Nishikawa, J. Nishida, R. Ookura, S. I. Nishimura, S. Wada, T. Karino, M. Shimomura, *Mater. Sci. Eng. C* **1999**, 8–9, 495–500.
- [7] T. Nishikawa, J. Nishida, R. Ookura, S. I. Nishimura, S. Wada, T. Karino, M. Shimomura, *Mater. Sci. Eng. C* **1999**, 10, 141–146.
- [8] M. Srinivasarao, D. Collings, A. Philips, S. Patel, *Science* **2001**, 292, 79–83.
- [9] S. Ludwigs, A. Boker, A. Voronov, N. Rehse, R. Magerle, G. Krausch, *Nat. Mater.* **2003**, 2, 744–747.
- [10] M. Tanaka, M. Takebayashi, M. Miyama, J. Nishida, M. Shimomura, *Bio-Med. Mater. Eng.* **2004**, 14, 439–446.
- [11] E. Bormashenko, R. Pogreb, O. Stanevsky, Y. Bormashenko, O. Gendelman, *Mater. Lett.* **2005**, 59, 3553–3557.
- [12] C. X. Cheng, Y. Tian, Y. Q. Shi, R. P. Tang, F. Xi, *Macromol. Rapid Commun.* **2005**, 26, 1266–1272.
- [13] D. Beattie, K. H. Wong, C. Williams, L. A. Poole-Warren, T. P. Davis, C. Barner-Kowollik, M. H. Stenzel, *Biomacromolecules* **2006**, 7, 1072–1082.
- [14] C. Gao, D. Yan, *Prog. Polym. Sci.* **2004**, 29, 183–275.
- [15] S. A. Jenekhe, X. L. Chen, *Science* **1999**, 283, 372–375.
- [16] M. Ornatska, S. Peleshanko, K. L. Genson, B. Rybak, K. N. Bergman, V. V. Tsukruk, *J. Am. Chem. Soc.* **2004**, 126, 9675–9684.
- [17] Y. F. Zhou, D. Y. Yan, *Angew. Chem.* **2004**, 116, 5004–5007; *Angew. Chem. Int. Ed.* **2004**, 43, 4896–4899.
- [18] D. Y. Yan, Y. F. Zhou, J. Hou, *Science* **2004**, 303, 65–67.
- [19] Y. H. Kim, O. W. Webster, *J. Am. Chem. Soc.* **1990**, 112, 4592–4593.
- [20] G. R. Newkome, C. N. Moorefield, G. R. Baker, M. J. Saunders, S. H. Grossman, *Angew. Chem.* **1991**, 103, 1207–1209; *Angew. Chem. Int. Ed. Engl.* **1991**, 30, 1178–1180.
- [21] H. B. Liu, A. Jiang, J. Guo, K. E. Uhrich, *J. Polym. Sci. Part A* **1999**, 37, 703–711.
- [22] J. F. G. A. Jansen, E. M. M. de Brabander-van den Berg, E. W. Meijer, *Science* **1994**, 266, 1226–1229.
- [23] C. H. Liu, C. Gao, D. Y. Yan, *Macromolecules* **2006**, 39, 8102–8111.